Zhang, Youqi; Miyamori, Yasunori; Kadota, Takanori; Saito, Takehiko

Long-term investigations of dynamic behavior of a pre-stressed concrete ballasted railway bridge

Published in:
Structures

DOI:
10.1016/j.istruc.2023.04.118

Published: 01/07/2023

Document Version
Publisher's PDF, also known as Version of record

Structures 53 (2023) 822–832

Contents lists available at ScienceDirect

Structures

journal homepage: www.elsevier.com/locate/structures

Long-term investigations of dynamic behavior of a pre-stressed concrete ballasted railway bridge

Youqi Zhang [a,*], Yasunori Miyamori [b], Takanori Kadota [c], Takehiko Saito [c]

[a] Department of Civil Engineering, School of Engineering, Aalto University, Finland
[b] Division of Civil Engineering, School of Engineering, Hokkaido University, Japan
[c] Department of Civil and Environment Engineering, Kitami Institute of Technology, Japan

ARTICLE INFO

Keywords:
Dynamic properties
Vibration experiment
Ballasted bridge
Environmental effect
Mode identification

ABSTRACT

Dynamic properties of civil structures such as natural frequencies, damping ratios, and mode shapes are essential parameters for evaluating the health condition of structures. However, dynamic properties are prone to be biased by environmental effects which may lead to fault structural health assessment. To investigate the environmental effect on the dynamic parameters of ballasted bridge, in this paper, a series of vibration experiments were performed on a multi-span pre-stressed concrete beam railway bridge. The dynamic properties of the bridge were identified and analyzed. In total, 9 experiments were conducted in 2 years. In the first 8 experiments, only sleepers and tracks had been removed. For the last experiment, the bridge was under destruction. The subsidiary components of the structure were destructed, and some holes were drilled on the slab for hoisting. The results show a clear seasonal variation in natural frequencies that in winters the natural frequencies reach local maximum values. Damping ratios show no clear variation regularity, indicating the complex correlation between the damping ratios and the environmental variation. Additionally, compression tests of concrete pieces of the slab were also conducted to investigate the degradation of material properties. The result of the compression tests indicates that there is approximately no degradation of compression strength of the concrete slab after the bridge was in service for several over 4 decades.

1. Introduction

Aging bridges have become a serious problem that threats social safety [1,2]. To solve this problem, vibration-based structural damage detection methods have been studied for several decades [3–5]. Theoretically, structural damages can directly lead to decreases in the local stiffness of the structure, which may cause variations of modal properties, such as natural frequencies, and mode shapes [6]. Thus, for vibration-based structural damage detection (SDD) methods [7,8], great attention has been paid to the modal properties of structures.

However, when applying modal-based SDD methods in actual bridges, the results tend to be biased by uncertainties. One of the main reasons is that the dynamic parameters, especially the natural frequencies, are easily biased by environmental effects, such as temperature, freeze, etc. To understand the environmental effect on the dynamic properties of structures, the dynamic properties of an RC slab were monitored by Xia et al. [9], and the effect of temperature and humidity is investigated. It is found that the natural frequencies decrease with the temperature or humidity increase. Lin et al. [10] the temperature effect on the natural frequency of a composite beam. Hu et al. [11] investigate the dynamic properties of a stress-ribbon footbridge. The result showed that temperature has a primary effect on the variations of frequencies. The correlation between the natural frequencies and the temperature of a cable-stayed bridge was analyzed by the support vector machine method by Ni et al. [12]. Xia et al. reviewed the temperature effect on civil structures and gave examples of a suspension bridge and a TV tower. The negative correlation between temperature and natural frequencies was also obtained [13]. Ubertini et al. [14] investigated the environmental effects on a tower and proposed a method to remove the effect. For the ballasted railway bridges, by monitoring the dynamic behavior of the bridge, the effect of frozen ballasts on the natural frequencies is found [15,16]. To briefly explain the mechanism of the environmental effect on the modal properties, the modulus of elasticity of the construction materials varies owing to environmental changes.

For the aging railway bridges, considering the material properties of ballasts distributed on the slab, the structural compositions tend to be

* Corresponding author.
E-mail address: youqi.zhang@aalto.fi (Y. Zhang).

https://doi.org/10.1016/j.istruc.2023.04.118
Received 31 October 2022; Received in revised form 5 April 2023; Accepted 28 April 2023
Available online 4 May 2023

more complex, leading to more complicated dynamic properties. However, articles about the dynamic properties of ballasted bridges [17–20] are still limited, especially the ballasted bridges in cold regions remain insufficiently investigated. Therefore, in this paper, a series of experiments were conducted on a pre-stressed concrete ballasted railway bridge to investigate the variations of the dynamic properties. In total 9 vibration experiments were carried out including the final experiment when the bridge was under destruction. An additional compression experiment on the test pieces of the bridge was also performed to investigate the degradation of the compression strength of the concrete. Note that this article is based on Chapter 2 of the first author's doctoral thesis [21]. Through the long-term investigation of the bridge, the dynamic behavior of the bridge in different environments was analyzed and summarized.

2. Bridge description

The ballasted bridge investigated in this study is a 5-span pre-stressed concrete beam bridge in Kitami City, Hokkaido, Japan. The bridge's construction was finalized in 1976. Kitami City and Ikeda County were connected by the bridge. Fig. 1 depicts a lateral perspective of the bridge's three spans, and Fig. 2 displays a general drawing of the bridge. For each span, the span length is 31.3 m, and the length of the deck is 32.02 m. The total length of the bridge is 158.8 m.

Fig. 3 illustrates the bridge's section views. The structure was built with wide girders on the outer sides of each span, as seen in Fig. 3 (a), and narrow girders in the middle of each span, as demonstrated in Fig. 3 (b). Girder sections differ at the left and right quarter points of each girder. Each span includes three cross beams at each quarter point. Walkways were extended from the side girders. On the edge of each walkway, handrails are also designed.

According to the terrain under the bridge, the three piers on the Ikeda side are taller than the pier on the Kitami side, as shown in Fig. 2. The superstructure of the bridge is supported at the two ends of each girder by the line-bearing supports shown in Fig. 4. Line-bearing support is a type of classical bridge support used in Japan. Technically, it allows the bridge to rotate and move in both longitudinal and vertical directions. However, in actual cases, owing to the high self-weight, vertical movement is generally not considered. Freedom of longitudinal movement meets the requirement of expansion caused by temperature change.

As illustrated in Fig. 5, the ballasts were uniformly distributed on the slab of all five spans. The sleepers and rails had been removed for several years because the bridge was out of operation. The ballasts, ballast stoppers, walkways, and handrails were removed in the final step before the bridge was completely deconstructed, as shown in Fig. 6. Several holes were drilled on the slabs to lift the bridge's superstructure during deconstruction, as shown in Fig. 7.

3. Setup of experiments

3.1. Vibration experiment

A series of vibration studies were conducted from November 2015 to December 2017 to evaluate the dynamic characteristics of the bridge. Table 1 displays the experimental timetable and the ballast state in each experiment. Multiple vibration tests were performed on each individual span in all the experiments. The first eight experiments (No. 1 - No. 8) in Table 1 were carried out on the bridge without a sleeper or track, as indicated in Fig. 5. The final experiment (No. 9) was carried out when the bridge was under deconstruction, and it had no sleeper, track, ballast, ballast stopper, walkway, or handrail. Hoisting holes were also drilled in the slab. The final state of the bridge in the last experiment can be viewed in Figs. 6-7.

The Imote2 wireless acceleration sensor system detected, recorded, and saved the bridge's free-damped vibration. As shown in Fig. 8, the original sensor consists of an SHM-H sensor board [22], an Imote2 communication board [23], a power supply board, and an antenna. The Imote2 communication board has an excellent algorithm to minimize the time synchronization error. Based on the second author's investigation [24], the accuracy of mode shape identification using Imote-2 is sufficient for SHM purposes. To add the waterproof feature to the sensor, all the essential components were installed in a plastic box, see Fig. 9. An extra battery box was also used to extend the sensor's battery life.

In No. 1, 3, and 4 experiments, 10 sensors were positioned symmetrically on the ballast stoppers in two rows (5 sensors 2 rows) in each span. For efficiency reasons, the number of sensors on each span was decreased to 6 in the No. 2 and No. 5–9 experiments, as illustrated in the sensor distribution map in Fig. 10. Because of its ease of use, the excitation technique was human jumping and landing. At the walkways' middle and quarter points, subjected to symmetric and asymmetric excitations were applied. The measuring time for each measurement was 30 s, with a sampling frequency of 280 Hz. Free damped vibration of the bridge corresponding to each excitation pattern was recorded.

The wireless sensor network was used to collect and transmit acceleration data to the computer. Because only impulse excitations were used, the bridge's dynamic responses were free-damped vibrations. Therefore, the peak-picking method was used for identifying natural frequencies. The mechanism of peak picking is that frequency response functions attain extreme values at natural frequencies. Then, the half-power bandwidth approach [25] was used to compute the damping ratios. Finally, the cross-spectrum approach [26] was used to estimate the mode shapes.

4. 3.2·Compression test of the test-piece

As introduced in Section 2, the bridge was drilled on its slab for

Fig. 1. The investigated bridge.

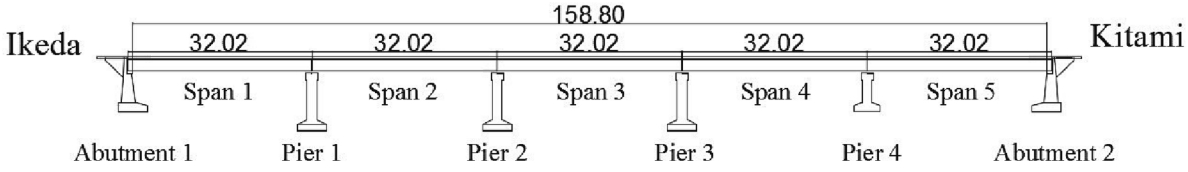

Fig. 2. Design and dimensions of the investigated bridge (Unit: m) [28].

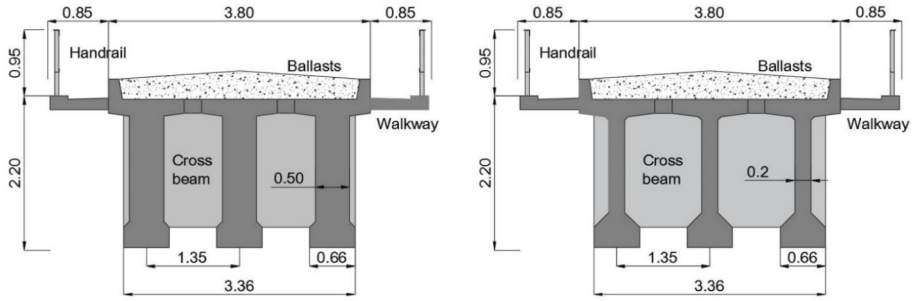

(a). two sides of each span (b). middle of each span

Fig. 3. Sectional views and dimensions of the bridge (Unit: m).

Fig. 4. Line-bearing support.

Fig. 5. Evenly distributed ballasts on the bridge.

Fig. 6. Bridge under destruction.

lifting. Cylindrical concrete samples were obtained by the drilling operations. As we know, it is normally impossible to directly take samples from in-service structures for material tests. Hence, these cylindrical concrete samples provide a rare opportunity to understand the degradation of material properties of a real bridge. The degradation of material properties can also affect the structural health state. Therefore, the compression tests were also presented in this article as additional information.

In total, the compression test on 3 concrete samples was conducted in our laboratory to estimate the compression strengths. Compared to the design compression strength, the degradation of material properties of the concrete was roughly evaluated.

5. Result

5.1. *Vibration experiments [21]*

In all the experiments, free-damped vibrations of the ballasted bridge

Fig. 7. Holes on the slab for lifting.

Table 1
Experimental schedule.

Experimental Number	Date (yyyy-mm-dd)	Ballast state
No. 1	2015–11-16	Wet
No. 2	2016–2-11	Frozen
No. 3	2016–8-18	Wet
No. 4	2016–10-18	Dry
No. 5	2016–11-29	Wet
No. 6	2017–2-3	Frozen
No. 7	2017–4-13	Wet
No. 8	2017–7-25	Dry
No. 9	2017–12-28	Removed

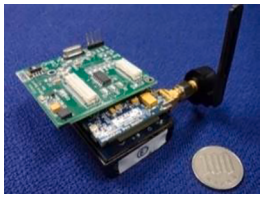

Fig. 8. Original wireless sensor [28].

Fig. 9. Updated vibration sensor.

were measured. Fig. 11 shows examples of the free-damped vibration data and corresponding frequency spectrums acquired from Ch. 0 installed on Span 3 in the No. 4 experiment. Fig. 11(a) and (b) represent the vibration excited by a symmetric impulse load on the middle point of Span 3, while Fig. 11(c) and (d) represent the vibration excited by a symmetric impulse load on the quarter point of Span 3. Owing to the different load locations, one more mode (the second bending mode) can be identified in Fig. 11 (d) than Fig. 11 (b) by the peak at 14.32 Hz.

Because of the relatively simplistic structure and load type (simply-supported girder bridge with impulse load), the natural frequencies

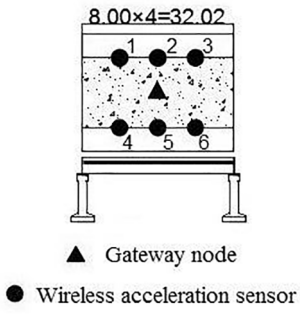

Fig. 10. Sensor distribution map.

were easily identified from the peaks in the frequency spectrums. Observing the identified natural frequencies in the multiple tests in each experiment, the natural frequencies were very concentrated. Using No.4 experiment (2016.10.18) on Span 3 as examples, the natural frequencies of mode 1 identified from the 4 tests with a symmetric load on the middle span were 4.0337 Hz, 4.0337 Hz, 4.0337 Hz, and 3.995 Hz, the natural frequencies of mode 2 identified were all 6.9051 Hz.

By applying the peak-picking method on the frequency spectrums of the vibration data, up to the natural frequencies 6 modes were identified in the 9 experiments, as summarized in Fig. 12. Then by using the half-power bandwidth method on the frequency spectrums of the vibration data, the damping ratios were calculated and visualized in Fig. 13. To understanding the identified 6 modes, the shape models were estimated using cross-spectrum method. Fig. 14 illustrates the mode shapes of Span 1 obtained from the No. 4 experiment as an example. The six identified vertical modes were 1st bending mode, the 1st torsional mode, the 2nd torsional mode, the 2nd bending mode, the 3rd torsional mode, and the 3rd bending mode. These modes are listed from lower to higher order.

In Figs. 12 and 13, some data were missing. The reason for the missing data of the first two modes on Span 5 on 2016–8-18 was battery problems. The missing results of modes 3–4 on 2015–11-6 (No. 1 experiment) were because of the missing vibration data with excitations on the quarter points. Then in the last experiment (2017–12-28, No. 9), the bridge was under destruction, owing to safety reasons, experiments were only performed on Spans 1 and 2, and only modes 1,2,4 and 6 were successfully excited.

In Fig. 12, the natural frequencies in each mode from the No.1 to No.8 experiments show a clear seasonal variation tendency that there are two local maximum peaks of the natural frequencies in the Februaries of 2016 and 2017. To find reasonable explanations for this phenomenon, we have carried out a series of investigations [16,27,28]. Because Hokkaido is in the northern hemisphere, the season in February is winter. Normally, the relatively high Young's modulus of concrete in winter caused by the low temperature is the main reason for this phenomenon, which can be proved by the approximate negative correlation between the average temperature on each experimental day and the natural frequency, as shown in Fig. 15, in which the left axis is the natural frequency of the first model of Span 1, and the right axis is the average temperature. However, the temperature gap between the No. 2 (2016-2-11) and No. 5 (2016-11-29) experiments was only 2 °C, as shown in Fig. 15. The 2 °C temperature difference could not lead to such a large natural frequency difference. Meanwhile, the frozen supports could be another possible reason to cause this phenomenon [29]. Based on our visual inspection, there was no ice or snow on the supports. The boundary condition of the bridge did not change. Therefore, great attention was paid to the frozen ballasts. In this series of experiments, three typical ballast states were obtained, dry, frozen, and wet, as shown in Fig. 16.

The dry ballast state shown in Fig. 16 (a) was presented in the No. 1 experiment. There was no rainfall during the week before the experiment. The moisture content of the ballasts was very low. In the No. 1

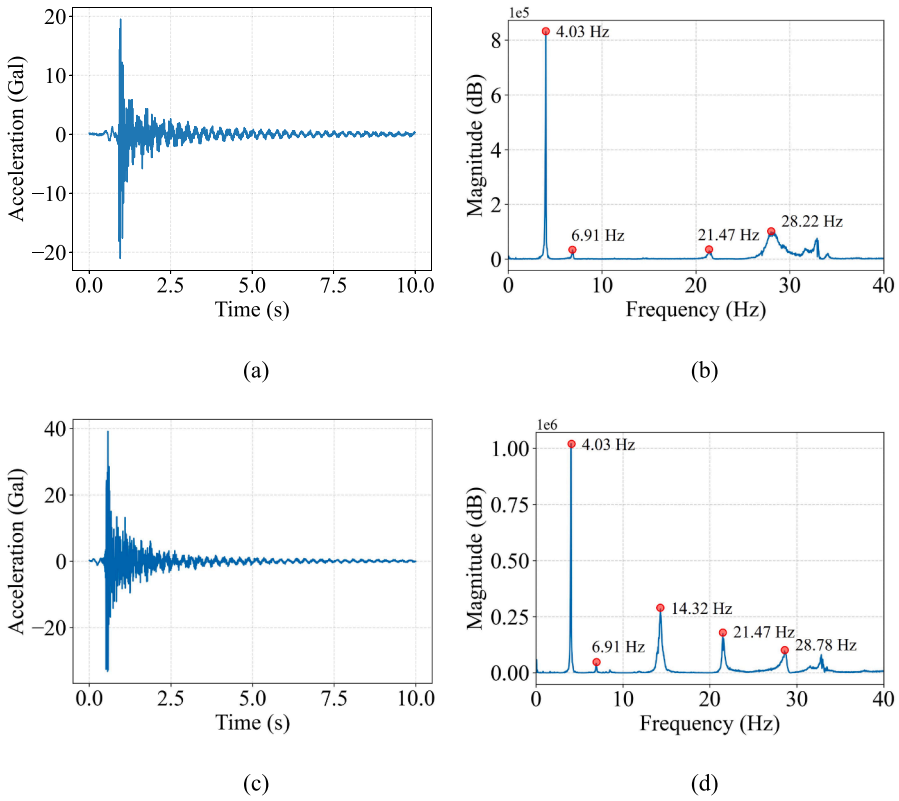

Fig. 11. Free damped vibration data and corresponding spectrums acquired from Ch. 0, Span 3, No.4 Experiment. (a) waveform excited by a symmetric load at the middle point of the span, (b) frequency spectrum of the vibration data shown in Fig. 11(a) with identified natural frequencies, (c) waveform excited by an asymmetric load at the quarter point of the span, (d) frequency spectrum of the vibration data shown in Fig. 11(c) with identified natural frequencies.

experiment, the dry ballasts were discrete with almost no adhesive effect. The No. 2 experiment demonstrated the frozen ballast state displayed in Fig. 16 (b). Ballasts were completely frozen. The ice filled the gaps between the ballasts and changed them into new composite material. Due to the unique climates in Hokkaido's winter, the ballasts experienced a special temperature variation process. The snow on the ballasts would melt into water and leak into the space inside the ballasts when the daily temperature varied around 0 °C. When it dropped to 0 °C, the seeping water would freeze. The ice that filled the area inside the ballasts would accumulate over a number of cycles in which the daily temperature varied around 0 °C. The material properties of the frozen ballasts would inevitably shift when the ice content increased to a comparatively high level. One could consider it a new composite material. According to this hypothesis, the ballasts serve as aggregate, and the ice serves as a filler. In the No. 5 experiment, the wet ballast state shown in Fig. 16 (c) was investigated. The ballasts were damp but not frozen. Ballasts may become more adhesive and feel less friction as their moisture levels increased. In contrast to freezing, the impact on natural frequency change was smaller.

Additionally, the natural frequencies of the final experiment (No. 9) were obtained in a significantly different bridge condition with no ballast, ballast stopper, walkway, or handrail. Meanwhile, many holes are drilled in the deck. To sum up, all the subsidiary components of the structure were removed, and even some structural damages were made on the slab. In these circumstances, the excitation positions of the No. 9 experiment were slightly adjusted to the inside areas for safety reasons. Thus, only 4 modes were identified: the 1st bending mode, the 1st torsional mode, the 2nd bending mode, and the 3rd bending mode, as shown in Fig. 12 (a), (b), (d), and (f). The 2nd and 3rd torsional were not sufficiently excited. The results show that the natural frequencies in the No. 9 experiment are much higher than the natural frequencies in other experiments. The reason should be that after the subsidiary components of the bridge were removed, especially the ballasts, the mass of the bridge was greatly reduced. The lower mass of the structure leads to higher natural frequencies. For the holes on the deck, theoretically, structural damages may decrease the natural frequencies since the stiffness of the bridge was reduced. However, the effect of the holes on the natural frequencies is much lower than the effect of removing the subsidiary components of the bridge on the natural frequencies. As a result, the natural frequencies during destruction increased greatly even though the slab was drilled with holes.

Meanwhile, Fig. 12 also shows another interesting phenomenon: the natural frequencies of internal Span 4 are higher than the other two internal Spans 2 and 3. In this case, the difference in span length during construction was not the main reason to cause this phenomenon because the 5 spans have the same designed length. One possible reason should be the different lengths of piers under the 3 internal spans. If one span and its supporting piers (or abutment) were considered as a frame structure as shown in Fig. 17, this phenomenon could be easily explained. The longer the supporting piers, the lower the natural frequencies. Span 4 was supported by Piers 3 and 4, and Pier 4 is obviously shorter than the other piers. Therefore, the natural frequencies of Span 4 are higher than those of Spans 2 and 3.

For the damping ratios shown in Fig. 13, through a general view, no clear regularity could be found within these data. The damping ratios did not show any apparent trend as the natural frequencies. The damping ratios varied independently from the seasonal change. One of the possible reasons for this phenomenon could be the high complexity of the ballasts. The differences between the ballasts lead to the different spaces and interaction mechanisms between ballasts which would directly affect the moisture content, fiction, and stickiness of the ballasts. Furthermore, with the onset of ice material in winter, the ballasts can be frozen, leading to more complex material properties. To sum up, all the mentioned factors can differ the amount of the absorbed and

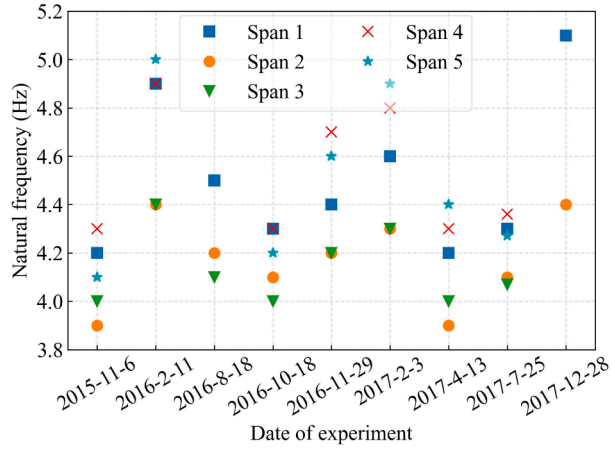

(a) 1st bending mode

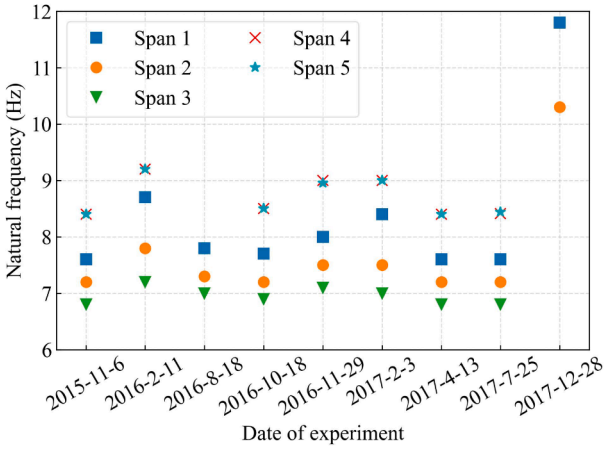

(b) 1st torsional mode

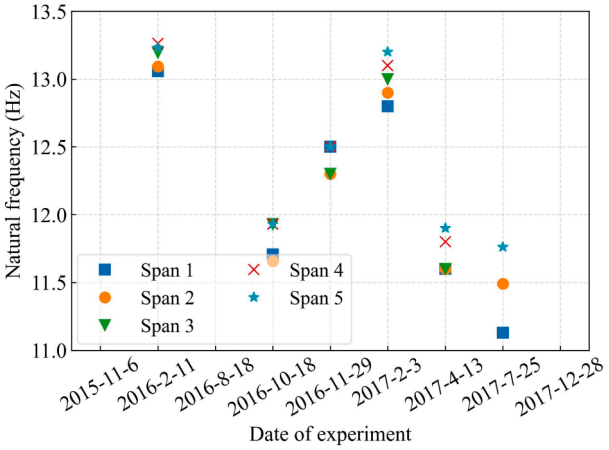

(c) 2nd torsional mode

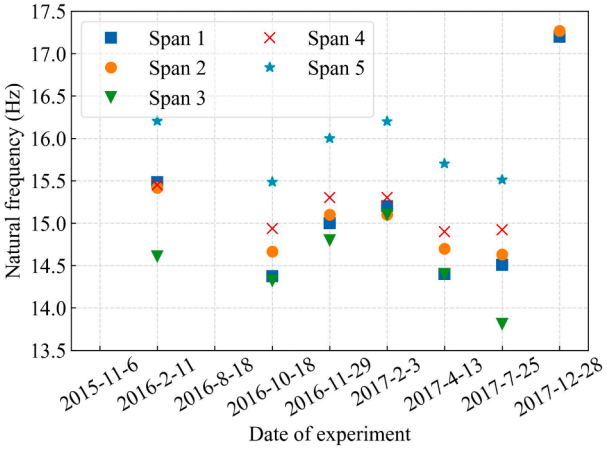

(d) 2nd bending mode

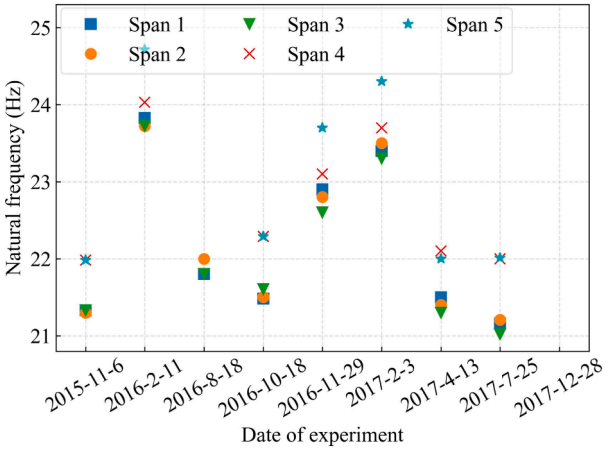

(e) 3rd torsional mode

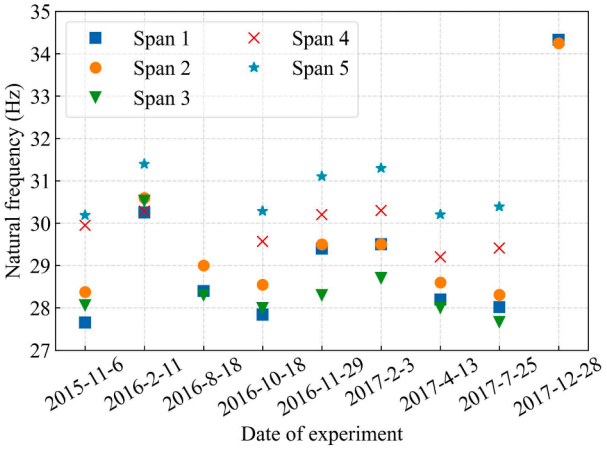

(f) 3rd bending mode

Fig. 12. Identified natural frequencies of the five spans.

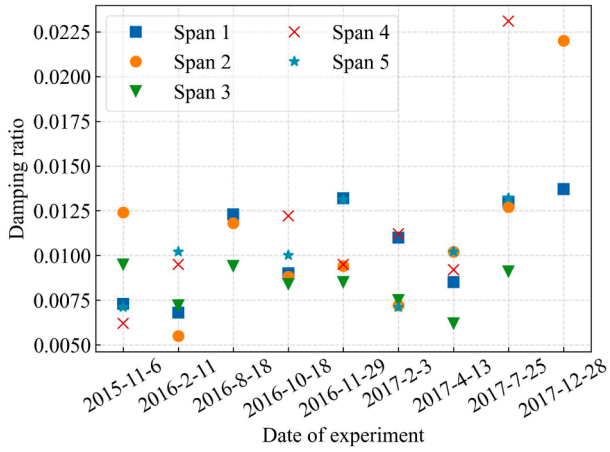

(a) 1st bending mode

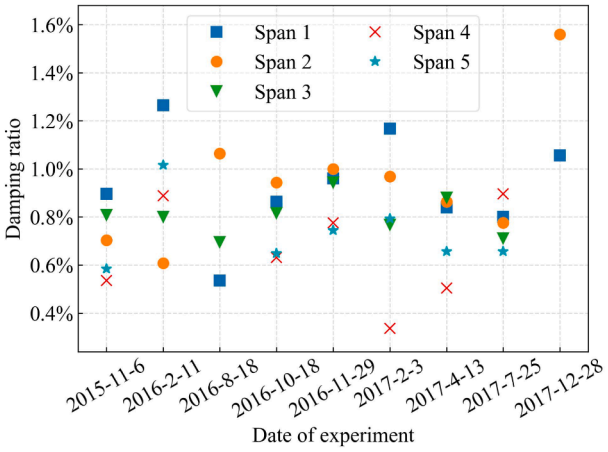

(b) 1st torsional mode

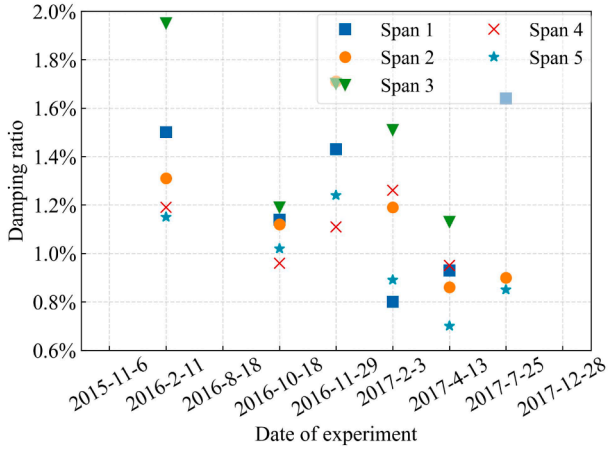

(c) 2nd torsional mode

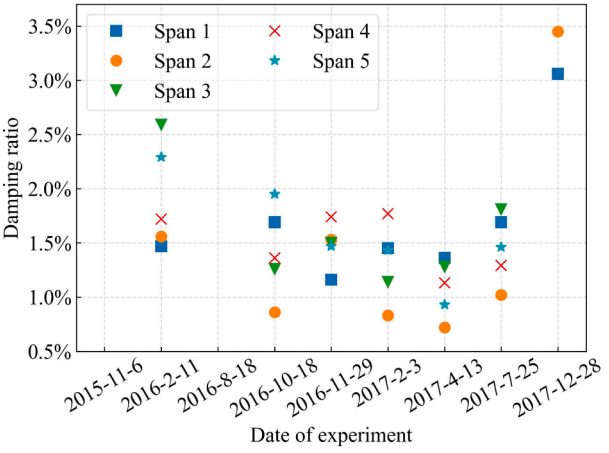

(d) 2nd bending mode

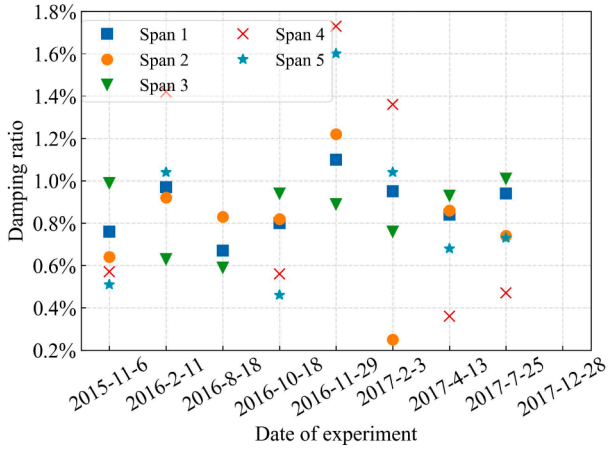

(e) 3rd torsional mode

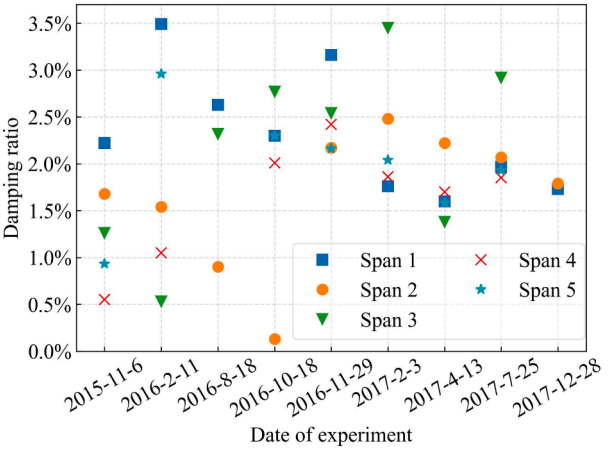

(f) 3rd bending mode

Fig. 13. Identified damping ratios of the five spans.

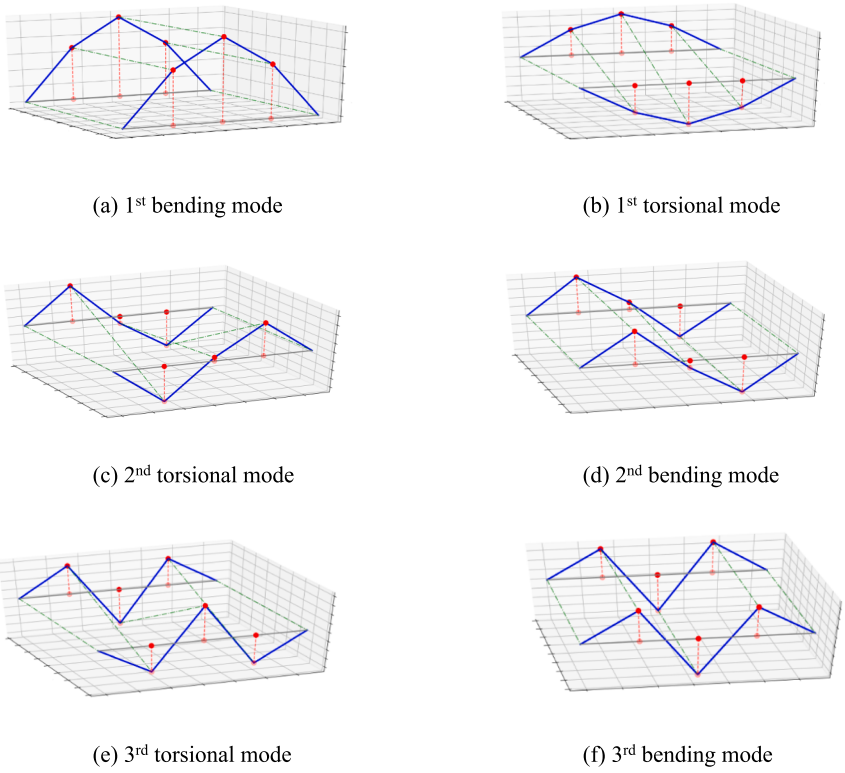

(a) 1st bending mode (b) 1st torsional mode

(c) 2nd torsional mode (d) 2nd bending mode

(e) 3rd torsional mode (f) 3rd bending mode

Fig. 14. Identified mode shapes of Span 1 obtained from the No. 4 experiment.

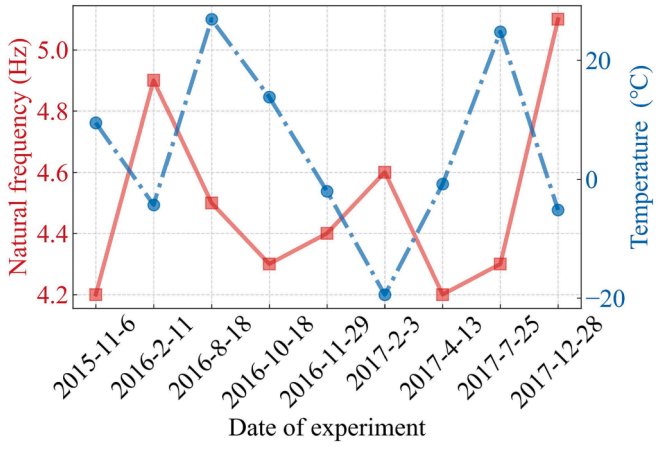

Fig. 15. Correlation of the average temperature of the experimental days and the natural frequency of mode 1 of Span 1.

damped vibration energy, leading to different identified damping ratios. For the last experiment (No. 9), the damping ratios of the 3 lower identified modes (the 1st bending mode, the 1st torsional mode, and the 2nd bending mode) increased obviously, which is far beyond the authors' expectations. Since the ballasts were taken removed, a decrease in the damping ratios was anticipated. The vibration's energy can be absorbed by the ballasts. Lower damping ratios were anticipated because the slab's ability to absorb energy is reduced without the ballasts. One possible reason for the increase in damping ratios is that by removing the subsidiary components of the bridge, the vertical forces on the supports were decreased, leading to lower frictions on the surfaces of the sliding bearing. If there were some motions on the supports, the energy of vibration was consumed in the relative movement of sliding

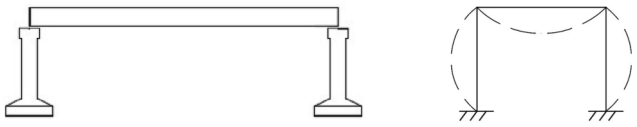

Fig. 17. Girder-pier frame structure.

(a) Dry (b) Frozen (c) Wet

Fig. 16. Three ballast states.

bearings. However, this assumption needs more study to prove.

Furthermore, another phenomenon on the identified mode shapes was found that they were not as stable as the natural frequencies. Two examples are shown in Figs. 18 and 19, corresponding to the amplitudes of the 1st bending mode shape of Span 2 in the No. 2 and No. 7 experiments. In total 7 tests were continuously performed on Span 2 with symmetric loads on the middle span in the No. 2 experiment. Similarly, in total 4 tests were continuously performed on Span 2 with symmetric loads on the middle span in the No. 7 experiment. The consistencies of the identified mode shapes in each individual experiment were evaluated using Modal Assurance Criterion (MAC):

$$MAC(r,q) = \frac{\left|\{\varphi_A\}_r^T\{\varphi_X\}_q\right|^2}{\left(\{\varphi_A\}_r^T\{\varphi_A\}_r\right)\left(\{\varphi_x\}_q^T\{\varphi_X\}_r\right)},$$

where φ_A and φ_X are two mode shape vectors to compare. According to the MAC values in Figs. 18 and 19, the consistencies of mode shapes are generally very high (over 0.98). However, when repeated several times, slightly lower consistencies may occur, such as 0.909 in Fig. 18 and 0.956 in Fig. 19 appeared. Therefore, this variation in the consistency of mode shapes may cause challenges in detecting very small structural damages using the mode shapes of the ballasted PC railway bridge.

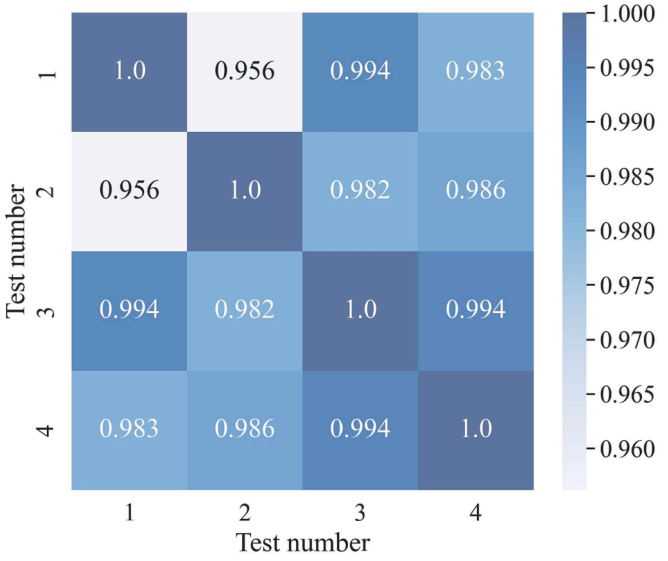

Fig. 19. MAC values of mode 1 from the 4 continuous tests on Span 2 in No. 7 Experiment.

5.2. Compression tests

As introduced in Section 2, the bridge was drilled on its slab for lifting. In total three cylindrical samples were taken to the laboratory for compression tests to investigate the longitudinal compressive load-bearing strengths. The information on the three cylindrical samples and the test results are shown in Table. 3. The three samples have the approximately same diameters but different heights in a range between 247 and 271 mm. A photo of the compression experiment is shown in Fig. 20.

The results show that the longitudinal compressive strengths of the three test pieces are 37.28 N/mm^2, 42.13 N/mm^2, and 39.83 N/mm^2 respectively. The mean longitudinal compressive strength of the three test pieces is 39.7 N/mm^2 with a very low standard deviation of 1.981 N/mm^2. Compared to the design compression strength of the concrete of 40 N/mm^2, the results of the sampling investigation show that after

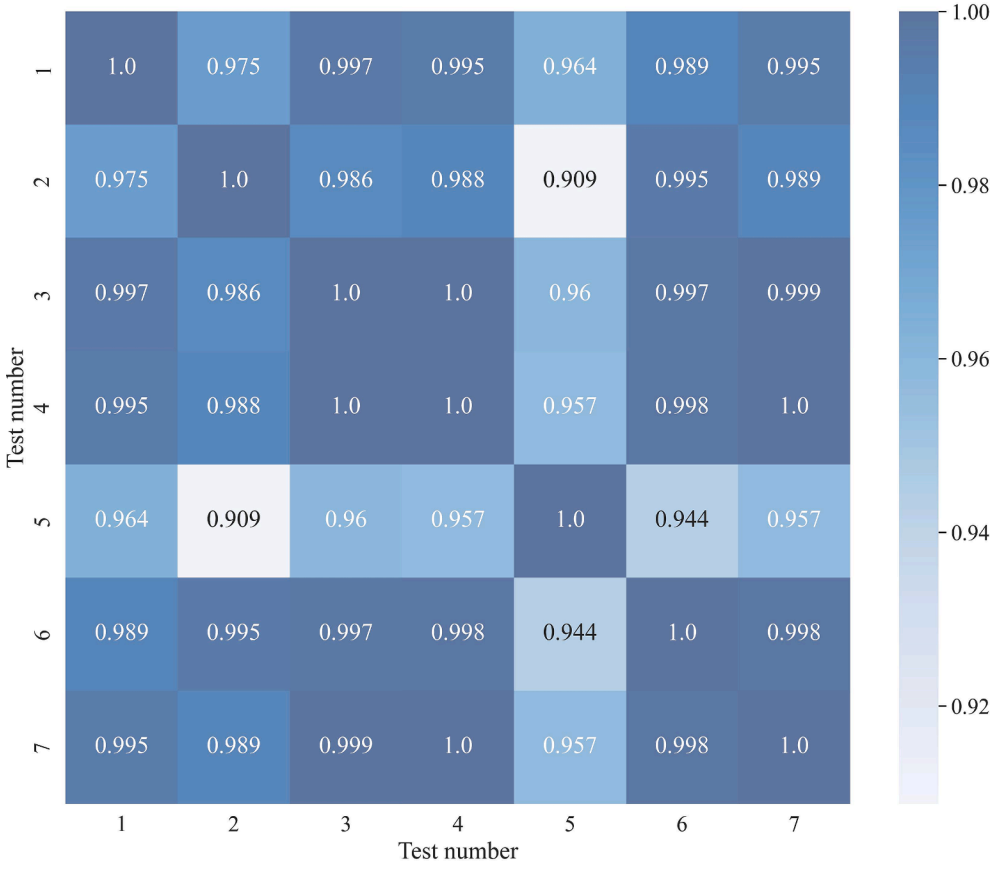

Fig. 18. MAC values of mode 1 from the 7 continuous tests on Span 2 in No. 2 Experiment.

Table 3
Result of the compression test of bridge pieces.

Number Unit	Diameter (mm)	Height (mm)	Mass (kg)	Maximum Load (N)	Longitudinal compressive strength (N/mm^2)	Standard Deviation (N/mm^2)	Mean longitudinal compressive strength (N/mm^2)	Coefficient of variation (%)
1	149.2	271.4	10.403	661,400	37.28	1.981	39.7	4.98
2	149.4	257.7	10.026	754,700	42.13			
3	149.4	247.6	9.491	717,400	39.83			

Fig. 20. A photo of the compression experiment of concrete sample.

decades of service, the compression strength of the concrete slab almost did not decrease, indicating the good health condition and durability of the concrete.

6. Conclusions

In this paper, a series of investigations of dynamic parameters of a multi-span ballasted pre-stressed concrete simply supported beam railway bridge were conducted over 2 years. Based on the results of the experiments, several conclusions are drawn as follows:

Firstly, for the ballasted bridge, a clear seasonal variation of natural frequencies is found. In winter, the natural frequencies of the bridge can be significantly increased by the frozen ballasts. The condition of ballasts changes dramatically in winter.

Secondly, for damping ratios, there is no obvious regularity of the damping ratio variation for the investigated ballasted bridge. No clear correlation between damping ratios and environmental conditions is found based on the results. After removing the subsidiary components of the bridge, the damping ratios of the lower modes increased notably.

Thirdly, the mode shapes of the ballasted PC railway bridge are not stable, even in the same environmental condition in the same experiment. Thus for the ballasted PC railway bridges, the mode shapes are not feasible to be an indicator to detect small damages.

Finally, when the bridge was damaged with several drilled holes on the slab, the natural frequencies of the bridge were also increased in the condition that all the subsidiary components of the bridge such as ballasts, ballast stoppers, walkways, and handrails were removed. Losing components greatly reduced the mass of the structure, which has a larger effect on natural frequencies than the drilling holes. Therefore, when using natural frequencies as a structural damage indicator, the changes in structural mass could not be ignored in the range of vibration modes measured in this experiment.

There are also some limitations in this study. The experimental results only qualitatively show some trends of variations of dynamic properties. The quantitative study of the correlation between the dynamic properties of the bridge and the environmental factors needs denser experiments. Moreover, the damping ratios in this study show no clear regularity. The complicated mechanism of damping ratio needs more effort to have a better understanding of the dynamic characteristics of the ballasted railway bridge.

Declaration of Competing Interest

The authors declare that they have no known competing financial interests or personal relationships that could have appeared to influence the work reported in this paper.

Acknowledgements

This research was financially supported by Japan Society for the Promotion of Science (JSPS) Grant-in-Aid for Scientific Research(C) Grant Number 15K06176, Japanese Government Scholarship (MEXT), and the Academy of Finland (decision number: 339493). The contributions of Mr. Yuta Shirakawa, Ms. Sanae Suzuki, Mr. Kaneyoshi Okada, Dr. Tomoyuki Yamazaki, Dr. Shunzo Kawajiri, and the Kitami City Government were greatly acknowledged.

References

[1] AASHTO, Bridging the gap-Restoring and rebuilding the nation's bridges, Washington (DC): American Association of State Highway and Transportation Officials, (2008).
[2] MLIT, White Paper On Land, Infrastructure, Transport And Tourism In Japan, 2015, Ministry of Land, Infrastructure, and Transport Tokyo, 2015.
[3] Farahani RV, Penumadu D. Damage identification of a full-scale five-girder bridge using time-series analysis of vibration data. Eng Struct 2016;115:129–39.
[4] Kumar PR, Oshima T, Yamazaki T, Mikami S, Miyamouri Y. Detection and localization of small damages in a real bridge by local excitation using piezoelectric actuators, Journal of Civil. Struct Health Monit 2012;2(2):97–108.
[5] Dilena M, Morassi A, Perin M. Dynamic identification of a reinforced concrete damaged bridge. Mech Syst Sig Process 2011;25(8):2990–3009.
[6] Adeli H, Jiang X. Intelligent infrastructure: neural networks, wavelets, and chaos theory for intelligent transportation systems and smart structures. CRC Press; 2008.
[7] He K, Zhu W. Structural damage detection using changes in natural frequencies: theory and applications. J Phys: Conf Ser, IOP Publishing 2011:012054.
[8] Yang Z, Wang L. Structural damage detection by changes in natural frequencies. J Intell Mater Syst Struct 2010;21:309–19.
[9] Xia Y, Hao H, Zanardo G, Deeks A. Long term vibration monitoring of an RC slab: temperature and humidity effect. Eng Struct 2006;28(3):441–52.
[10] Lin B, Xie T, Xu M, Li Y, Yang J. Natural frequencies and dynamic responses of rotating composite non-uniform beams with an elastically root in hygrothermal environment. Compos Struct 2019;209:968–80.
[11] Hu W-H, Caetano E, Cunha Á. Structural health monitoring of a stress-ribbon footbridge. Eng Struct 2013;57:578–93.
[12] Ni Y, Hua X, Fan K, Ko J. Correlating modal properties with temperature using long-term monitoring data and support vector machine technique. Eng Struct 2005;27:1762–73.
[13] Xia Y, Chen Bo, Weng S, Ni Y-Q, Xu Y-L. Temperature effect on vibration properties of civil structures: a literature review and case studies. J Civ Struct Heal Monit 2012;2(1):29–46.
[14] Ubertini F, Comanducci G, Cavalagli N, Pisello AL, Materazzi AL, Cotana F. Environmental effects on natural frequencies of the San Pietro bell tower in Perugia, Italy, and their removal for structural performance assessment. Mech Syst Sig Process 2017;82:307–22.
[15] Gonzales I, Ülker-Kaustell M, Karoumi R. Seasonal effects on the stiffness properties of a ballasted railway bridge. Eng Struct 2013;57:63–72.
[16] Zhang Y, Miyamori Y, Kadota T, Saito T. Investigation of seasonal variations of dynamic characteristics of a concrete bridge by employing a wireless acceleration sensor network system. Sensors & Materials 2017;29:165–78.
[17] Rigueiro C, Rebelo C, da Silva LS. Influence of ballast models in the dynamic response of railway viaducts. J Sound Vib 2010;329:3030–40.
[18] Aloisio A, Rosso MM, Alaggio R. Experimental and Analytical Investigation into the Effect of Ballasted Track on the Dynamic Response of Railway Bridges under Moving Loads. J Bridg Eng 2022;27:04022085.

[19] Chordà-Monsonís J, Romero A, Moliner E, Galvín P, Martínez-Rodrigo M. Ballast shear effects on the dynamic response of railway bridges. Eng Struct 2022;272:114957.
[20] Rebelo C, da Silva LS, Rigueiro C, Pircher M. Dynamic behaviour of twin single-span ballasted railway viaducts—Field measurements and modal identification. Eng Struct 2008;30:2460–9.
[21] Zhang Y. Vibration-based Structural State Identification by using Deep Learning Method. Kitami Institute of Technology 2019.
[22] Ishmp S. Board High-Sensitivity Accelerometer Sensor Board Datasheet and. User's Guide 2009.
[23] Crossbow, Imote2 High-Performance Wireless Sensor Network Node, 2007.
[24] Nagayama T, Sim SH, Miyamori Y, Spencer BFJ. Issues in structural health monitoring employing smart sensors. Smart Struct Syst 2007;3(3):299–320.
[25] Papagiannopoulos GA, Hatzigeorgiou GD. On the use of the half-power bandwidth method to estimate damping in building structures. Soil Dyn Earthq Eng 2011;31(7):1075–9.
[26] Liou CY, Jeng T-S. The determination of mode shapes from modern cross-spectral estimates. Mech Syst Sig Process 1989;3(3):291–303.
[27] Zhang Y, Miyamori Y, Shirakawa Y, Saito T. Significant Dynamic Parameter Variations of a Ballasted Railway Bridge Investigated by Employing a Wireless Smart Senor Network System. Proceedings in The 13th International Workshop on Advanced Smart Materials and Smart Structures Technology (ANCRiSST2017). Japan: The University of Tokyo; 2017.
[28] Zhang Y, Miyamori Y, Oshima T, Mikami S, Saito T. Effect of Ballast State on Natural Frequencies of a Multi-Span Ballasted Prestressed Concrete Railway Bridge. In: Proceeding in Structural Health Monitorings of Intelligent Infrastructure Conference 2017 (SHMII 8), Brisbane, Australia; 2017. p. 2017.
[29] Alampalli S. Influence of in-service environment on modal parameters, Proceedings-SPIE the international society for optical engineering. Citeseer 1998:111–6.